REPORT DOCUMENTATION PAGE

Form Approved
OMB No. 0704-0188

1. REPORT DATE *(DD-MM-YYYY)*	2. REPORT TYPE	3. DATES COVERED *(From - To)*
05-02-2007	REPRINT	

4. TITLE AND SUBTITLE
Analysis of the Electrospray Plume from the EMI-Im Propellant Externally Wetted on a Tungsten Needle

5a. CONTRACT NUMBER

5b. GRANT NUMBER

5c. PROGRAM ELEMENT NUMBER
61102F

6. AUTHOR(S)
Y. Chiu, G. Gaeta, T.R. Heine, R.A. Dressler and D.J. Levandier*

5d. PROJECT NUMBER
2303

5e. TASK NUMBER
RS

5f. WORK UNIT NUMBER
A1

7. PERFORMING ORGANIZATION NAME(S) AND ADDRESS(ES)
Air Force Research Laboratory/VSBXT
29 Randolph Road
Hanscom AFB MA 01731-3010

8. PERFORMING ORGANIZATION REPORT NUMBER
AFRL-VS-HA-TR-2007-1009

9. SPONSORING / MONITORING AGENCY NAME(S) AND ADDRESS(ES)

10. SPONSOR/MONITOR'S ACRONYM(S)

11. SPONSOR/MONITOR'S REPORT NUMBER(S)

12. DISTRIBUTION / AVAILABILITY STATEMENT
Approved for Public Release; Distribution Unlimited

*Institute for Scientific Research, Boston College, Chestnut Hill, MA

13. SUPPLEMENTARY NOTES
REPRINTED FROM: 42nd AIAA/ASME/SAE/ASEE Joint Propulsion Conference and Exhibit, 9-12 Jul 06, Sacramento, CA (AIAA 2006-5010)

14. ABSTRACT

The room temperature ionic liquid propellant, 1-ethyl-3-methylimidazolium bis(trifluoromethylsulfonyl)imide (EMI-Im) is being tested for the NASA DRS-ST7 mission. A capillary thruster configuration is planned for ST7, and time-of-flight experiments have shown that the spray of EMI-Im produces a mixture of primarily droplets and low levels of ions, resulting in a low specific impulse. Recently, pure ion emission was achieved for EMI-Im in a wetted needle thruster, suggesting that this propellant, which has passed all space-environmental exposure tests, may also be a candidate for high specific impulse missions. The use of wetted tips raises the question whether electrochemistry at the liquid-metal interface causes significant propellant fouling that will ultimately result in performance degradation due to the significantly longer propellant metal interaction times in comparison with the capillary design and the higher flow rates. Electrochemical fouling can be mitigated through a polarity alternation approach, which adds complexity to the power processing unit.

15. SUBJECT TERMS
Ionic liquid, Electrospray thruster, Plume properties, Mass spectrometry, Ethyl-methyl-immidazolium ion, Nanojet

16. SECURITY CLASSIFICATION OF:			17. LIMITATION OF ABSTRACT	18. NUMBER OF PAGES	19a. NAME OF RESPONSIBLE PERSON
a. REPORT	b. ABSTRACT	c. THIS PAGE			R. Dressler
UNCLAS	UNCLAS	UNCLAS	SAR		19b. TELEPHONE NUMBER *(include area code)* 781-377-2332

42nd AIAA/ASME/SAE/ASEE Joint Propulsion Conference & Exhibit
9 - 12 July 2006, Sacramento, California

AIAA 2006-5010

Analysis of the Electrospray Plume from the EMI-Im Propellant Externally Wetted on a Tungsten Needle

Yu-Hui Chiu*, Geraldine Gaeta†, Thomas R. Heine‡, Rainer A. Dressler§
Air Force Research Laboratory, Space Vehicles Directorate, Hanscom AFB, Massachusetts, 01731

and

Dale J. Levandier**
Boston College, Institute for Scientific Research, Chestnut Hill, Massachusetts, 02159

The room temperature ionic liquid propellant, 1-ethyl-3-methylimidazolium bis(trifluoromethylsulfonyl)imide (EMI-Im) is being tested for the NASA DRS-ST7 mission. A capillary thruster configuration is planned for ST7, and time-of-flight experiments have shown that the spray of EMI-Im produces a mixture of primarily droplets and low levels of ions, resulting in a low specific impulse. Recently, pure ion emission was achieved for EMI-Im in a wetted needle thruster, suggesting that this propellant, which has passed all space-environmental exposure tests, may also be a candidate for high specific impulse missions. The use of wetted tips raises the question whether electrochemistry at the liquid-metal interface causes significant propellant fouling that will ultimately result in performance degradation due to the significantly longer propellant metal interaction times in comparison with the capillary design and the higher flow rates. Electrochemical fouling can be mitigated through a polarity alternation approach, which adds complexity to the power processing unit. Mass spectrometric experiments have the ability to identify electrochemical byproducts among the electrospray plume ions. We have conducted mass spectrometric, retarding potential, and angular distribution measurements for ions emitted from EMI-Im when sprayed from a wetted tungsten needle at nominal extraction voltages of ~1 kV. The angularly resolved measurements indicate that the spray comprises a mixture of droplets and ions, with the droplets concentrated in the center of the spray. The major ionic species identified are $EMI^+(EMI\text{-}Im)_n$ and $Im^-(EMI\text{-}Im)_n$, with $n = 0,1,2$ in the positive and negative polarities, respectively. The retarding potential analysis indicates that all major ions are formed at or near the needle potential. A small amount of fragment ions is observed that may be attributed to electrochemical degradation. We will present the time evolution of these fragment ions when operated in a continuous polarity mode in comparison with an alternating polarity approach.

I. Introduction

Room temperature ionic liquids (RTILs) are ideal propellants for electrospray thrusters due to their unique physical and chemical properties, namely high conductivity and negligible vapor pressure. The electrospray of some RTILs produces purely ionic emission, while others are discovered to emit an ion-droplet mixture. When an ionic liquid electrospray thruster is operated in a pure ionic emission mode, it resembles the performance of a field emission thruster. It has been proposed that pure ionic emission can be achieved by RTILs of specific physical

* Task Scientist, Space Vehicles Directorate, AFRL/VSBXT, 29 Randolph Road, Hanscom AFB, MA 01731. AIAA Member.
† Space Scholar, Space Vehicles Directorate. AIAA Member.
‡ First Lieutenant, Space Vehicles Directorate.
§ Task Scientist, Space Vehicles Directorate. AIAA Member.
** Staff Scientist, Institute for Scientific Research.

properties, such as high conductivity (K) and high surface tension (γ). Furthermore, the thruster must be operated with a low propellant flow rate (Q).[1,2]

The air stable room temperature ionic liquid, 1-ethyl-3-methylimidazolium bis(trifluoromethylsulfonyl)imide (EMI-Im), passed space environmental tests for the NASA's Space Technology 7- Disturbance Reduction System Mission (ST7-DRS), a demonstration of precision spacecraft positioning control.[3,4] Time-of-flight (TOF) experiments conducted for capillary configurations have shown that the electrospray of EMI-Im produces a mixture of primarily droplets and low levels of ions.[4,5] Recently, Lozano reported that the pure ionic emission of EMI-Im can be achieved via an externally wetted needle thruster.[6] This suggests that EMI-Im could also be a candidate for high specific impulse missions. Unlike the capillary thruster, where the flow rate control is regulated by pressure, the flow rate of an externally wetted needle depends primarily on the wetting property of the needle and the size of the needle.[7] In addition, the external wetting approach facilitates the electrospray of viscous ionic liquids.

It is also known that electrochemical reactions associated with the electrospray of ionic liquids could result in the propellant fouling. Lozano and Martínez-Sánchez demonstrated that electrochemical fouling could be suppressed using an alternating polarity approach for the EMI-BF_4 ionic liquid.[8] The ST7 electrospray thruster is operated in a positive dc mode, and has survived over 3,000 hours of operation without stability problems.[9] This raises the question why electrochemical propellant fouling is not affecting the EMI-Im propelled engine, since EMI-Im and EMI-BF_4 have very similar electrochemical windows.[10] One plausible explanation is that the electrochemical reaction products are carried out of the system by the high propellant flow rate and the large charged droplets.

Mass spectrometric measurements of field evaporated ions provides complementary information and improved resolution in relation to the more frequently applied TOF approach in identifying the ionic species.[11,12] The angular distribution of emitted charges is an important parameter with respect to beam collimation considerations, but also with respect to spacecraft integration. Angular measurements coupled with retarding energy analysis could provide information on the ion field evaporation mechanism by identifying the ion emission regions, such as the neck and jet of the conejet illustrated in Fig. 1. In the present work, we report measurements of angular distributions of mass and energy resolved positive and negative ions produced in the electrospray of EMI-Im via an externally wetted tungsten needle, operated at an alternating polarity of 1 Hz. To investigate if there are electrochemical products formed, we will compare the results of alternating polarity to those of a dc operation.

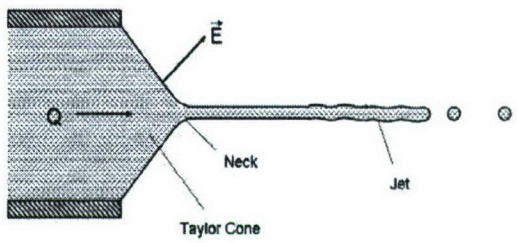

Figure 1. Illustration of a conejet.

II. Experimental

Figure 2 shows a schematic diagram of the apparatus. The thruster needle is comprised of a 20 mil diameter tungsten wire which is modified by following the chemical etching procedure described in Ref. 7. A typical tip size of the needle is ~20 μm. A short piece of 10 mil diameter tungsten wire is spot welded ~3 mm from the tip. This forms a junction that serves as the propellant reservoir. Prior to placing the thruster needle in the vacuum chamber, the needle tip is first heated and then a drop of EMI-Im propellant is deposited on the wire junction and propellant is spread to the tip. The unwetted end of the needle is then mounted in a copper cylinder block to which the electrical, heating and temperature sensing connections to the needle are made. The needle tip is located in the entrance plane of the extractor orifice, which has a diameter of 1.5 mm. The needle assembly, consisting of an aligned thruster needle and extractor, is rotatable with respect to the thrust axis, i.e., the axis of the apparatus, while the tip remains stationary during the rotation. The plane of the rotation is in the xz plane with maximum accessible angles of ± 45° with respect to the thruster axis, z. The extraction voltage, ± 1.05 kV, is alternated at 1 Hz. The needle potential floats at an absolute voltage of 500 V, while the extractor is held at 550 V of the opposite polarity. The needle potential is chosen to optimize resolution and transmission of ions in the mass spectrometer. The source and mass spectrometer/detector vacuum chambers are evacuated by 250 l/sec turbo molecular pumps, which typically achieve a base pressure of ~ 1 x 10^{-7} and 5 x 10^{-8} Torr, respectively.

The electrospray plume is first sampled at a near-field target, consisting of three devices mounted orthogonal to the beam on a linear translation manipulator: a Faraday cup assembly with an entrance aperture of 6 mm, a quartz crystal microbalance (QCM; XTM/2, Inficon) with the same size aperture, and a cylindrical lens element. Though a portion of the whole beam is sampled in the near-field target without prior focusing, the measured total charge and deposition registered on the QCM, as a function of thruster angle, serves as a qualitative guide for estimating the average specific charge. The time dependence of the thruster current level registered on the Faraday cup is used to monitor stability of emission at the specific applied voltages. The typical measured on-axis current level is ~ 40 nA for either polarity. When the cylindrical lens element is placed on-axis, the beam passes a 3 mm diameter aperture. After the aperture, the sampled portion of the beam is focused and injected into a quadrupole mass filter (3/8" diameter rod, Extrel ABB) using a set of ion lenses. The mass filter can be operated in either rf-only all pass, single mass selection, and mass scanning modes.[11] Following the mass filter is a set of three grids where the potential of the middle grid is scanned for obtaining the retarding energy potential for a mass-selected ion. An off-axis channeltron detector is used for positive and negative ion detection. The positive and negative ion mass spectral data acquisition is synchronized with the corresponding half-cycle of the applied 1 Hz alternating voltages. The laboratory angular distribution is obtained by recording ions that pass through the circular aperture of 3 mm diameter, situated 57 mm from the needle tip, as the thruster angle varies. The half angle of the solid angle of acceptance is ~3°. Positive and negative ion mass spectra are recorded as a function of thruster angle. Retarding potential analyses are performed for individual selected ion masses produced at selected thruster angles for both ion polarities.

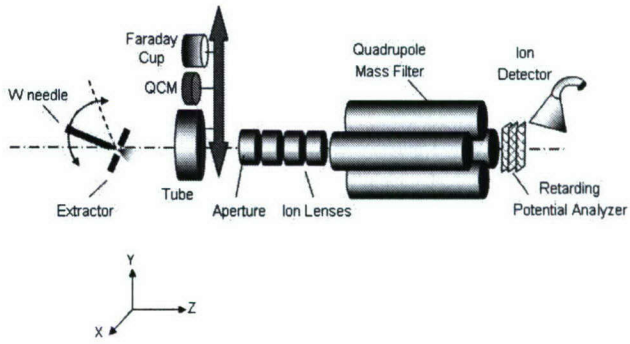

Figure 2. Schematic diagram of the mass spectrometric experiment.

III. Results

A. Alternating polarity mode

Figure 3 shows a series of positive ion mass spectra recorded in an alternating polarity mode as a function of thruster angle ranging from +25° to -25°. The zero angle points to the thruster axis. Displayed along the mass axis

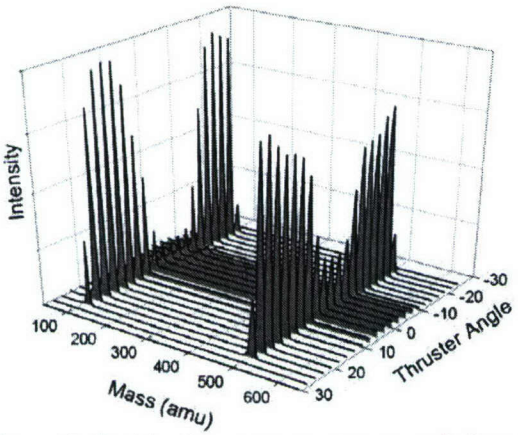

Figure 3. Positive ion mass spectra recorded as a function of thruster angle.

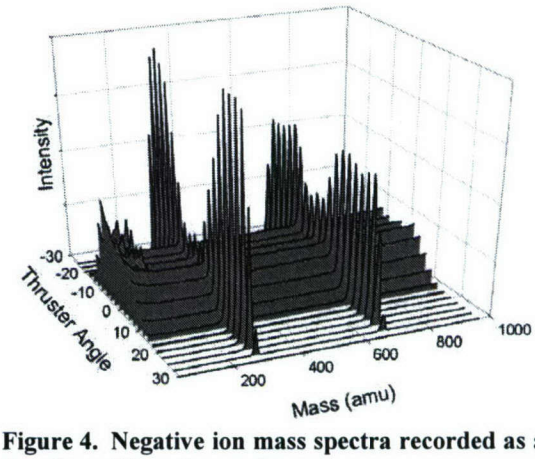

Figure 4. Negative ion mass spectra recorded as a function of thruster angle.

are two main ion peaks at 111 and 502 amu. They are assigned to the EMI^+ and $EMI^+(EMI\text{-}Im)$ ions, respectively. A much weaker peak attributed to the $EMI^+(EMI\text{-}Im)_2$ ion is also observed but not shown in Fig. 3. At small angles, a nearly constant level of background appears in the mass spectra. Small amounts of trace ions are also present at small angles. These mass peaks are at 78, 148, and 283 amu. Note that the accuracy in the mass determination is ±4 amu due to the limited data points. Figure 4 shows the corresponding angular distribution of negative ion mass spectra observed as a function of thruster angle. Two main negative ion peaks at 280 and 671 amu are identified as Im^- and $Im^-(EMI\text{-}Im)$ ions, respectively. Not shown in Fig. 4 are small amounts of $Im^-(EMI\text{-}Im)_2$. Again, significant background signal is observed at small angles. The background appears to be more prominent than that of the positive polarity. Also present at small angles are negative ion peaks at 87 and 115 amu with weak intensity. Figure 5 plots the deposition registered on the QCM as a function of thruster angle while the thruster is operated at a negative polarity. The mass flow angular distribution is consistent with the background in Fig. 4. The mass spectral background is likely due to the high m/q ions, such as droplets, which the quadrupole mass filter cannot discriminate against. The average q/m values derived from the ratio between QCM and Faraday cup measurements are 3960 and 5679 C/Kg for positive and negative ions, respectively, which corresponds to an average m/q > 24,000 amu for positive ions and > 16,800 amu for negative ions per charge. The similarity in the registered mass flow for both polarities implies that the different relative intensities between ion and droplets for the negative and positive polarities can be attributed to different detector sensitivities for the droplets with different charge polarity.

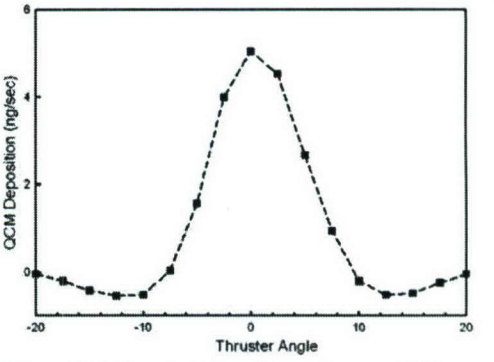

Figure 5. The angular dependence of the mass flow as measured on the QCM at negative polarity.

The retarding potential curve obtained for the Im^- ion while the thruster is on-axis is shown in Fig. 6. The open symbol and the solid line represent the raw and smoothed data, respectively. Two step-like features are clearly seen in the retarding potential curve. Plotted in the insert chart is the corresponding energy distribution of the Im^- ions on-axis. The energy distribution is obtained from the derivative of the smoothed retarding potential curve. Two main peaks are observed in the energy distribution: one intense, narrow peak with a width of ~30 eV centered at ~500 eV and another broader peak centered at ~320 eV. Figure 7 shows the retarding potential curve for negative ions produced on axis

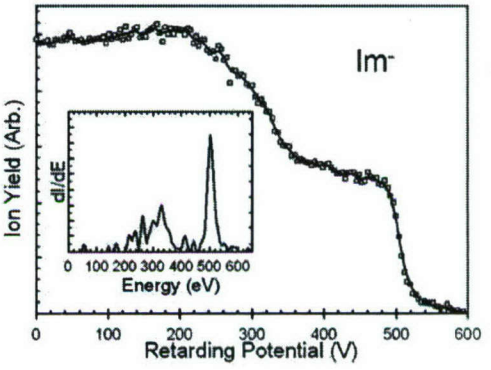

Figure 6. The retarding potential curve measured for Im^- on axis. The insert is the corresponding energy distribution.

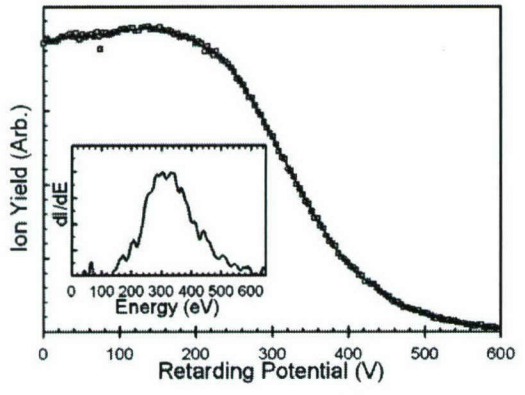

Figure 7. The retarding potential curve measured for high negative m/q particles. The insert is the corresponding energy distribution per charge unit.

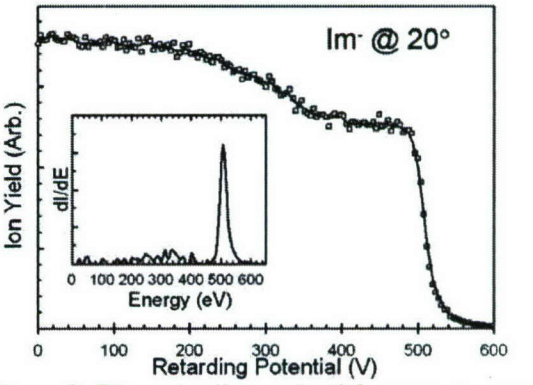

Figure 8. The retarding potential curve measured for Im^- at an angle of ~ 20°. The insert is the corresponding energy distribution.

while setting the mass filter to only allow the passage of high m/q particles (≥ 1200 amu). The insert chart is the corresponding energy distribution which exhibits a single broad peak centered at ~320 eV per charge unit. The retarding potential curve and energy distribution of Im^- at an angle of +20° is shown in Fig. 8. The energy distribution shows two peaks centered at ~500 eV and ~320 eV, the latter broader peak having a lower relative intensity than that of Im^- on axis.

The retarding potential curve and energy distribution of EMI^+ ions observed on-axis are shown in Fig. 9. Figure 10 shows the retarding potential curve and energy distribution of the EMI^+ ion at a large angle of ~18°.

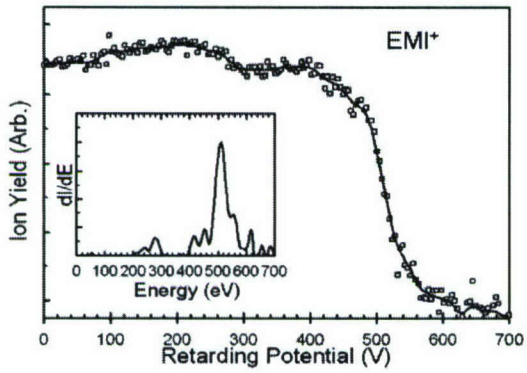

Figure 9. The retarding potential curve measured for EMI^+ on-axis. The insert is the corresponding energy distribution.

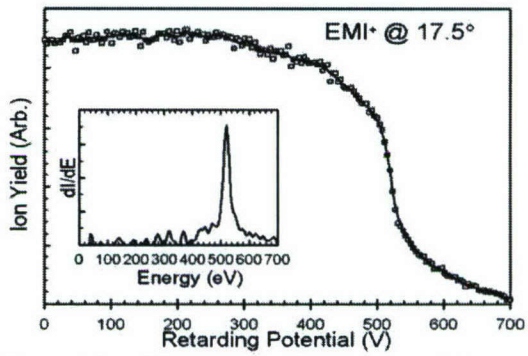

Figure 10. The retarding potential curve measured for the EMI^+ ion at an angle of ~ 17.5°. The insert is the corresponding energy distribution.

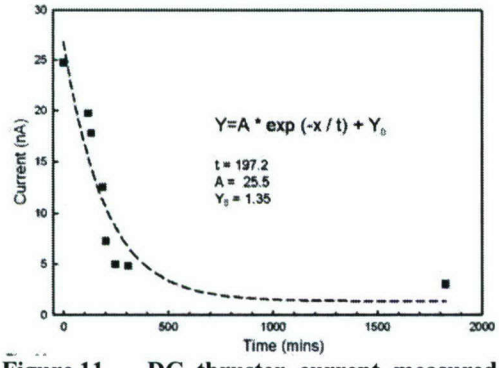

Figure 11. DC thruster current measured on-axis as a function of time.

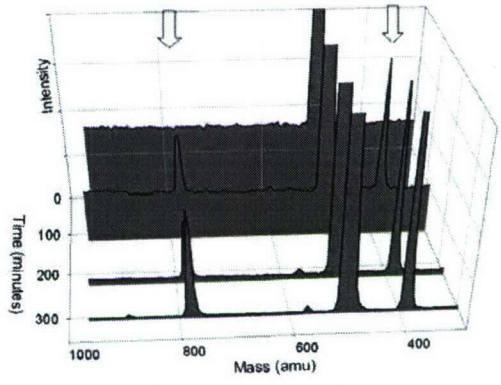

Figure 12. Time evolution of positive ion mass spectra taken at dc operation conditions.

B. DC Operation

The currents of the thruster outputs for both polarities were monitored as a function of time, using the near-field Faraday cup at a fixed thruster angle, near zero degrees. At several time intervals, ion mass spectra for both polarities were recorded. The observed output current was constant while operating the thruster in the negative ion mode. However, in the positive ion mode, the current output decreased with time. Figure 11 shows the measured output current as a function of time. The dashed line indicates a first order exponential decay fit and the associated fitting parameter values. Figure 12 plots positive ion mass spectra taken at several time intervals. The arrows point to two new peaks that grew in with time. These respective masses are 391 and 783 amu. Note that the background level also decreases with time. Interestingly, when switching back to alternating polarity mode after the dc mode tests, the current returns instantly to its original level and the excess ion masses are no longer observed in the mass spectra.

IV. Discussion

The angular measurements indicate that the intensities of the main $EMI^+\{[EMI][Im])\}_n$ and $Im^-\{[EMI][Im])\}_n$ ions observed, n = 0-2, are peaked at an off-axis angle of ~18°, while the droplets are found on-axis with a narrower distribution. These main ions are also observed by Lozano[6] and follow a similar trend to those observed for the electrospraying of EMI-BF_4 and EMI-NO_3.[12] In contrast to Lozano's TOF experiments, where the pure ionic emission of EMI-Im was observed, the present study observes a mixed ion-droplet regime. While both experiments use externally wetted needles, a source of the discrepancy could be the tip geometry. Indeed, in our earlier experiments using tips with larger curvature, a predominant droplet fraction was observed from EMI-Im. It is likely that the smaller tip curvature and the overall needle shape leading to the tip reduce the flow rate, thus pushing the thruster towards the pure ionic emission regime. As the flow rate increases, Gamero-Castaño et al have shown that the electrospray of EMI-Im produces a mixture of primarily droplets and low levels of ions from a capillary needle.[4]

As illustrated in Fig. 1, sources of ion emission for a conejet mode include the neck region, the tip of the jet, and the droplets. The mass-resolved energy distributions in conjunction with angular measurements allow the distinction for the ion emission sources. The observation of the droplets on-axis and ions off-axis is consistent with the hydrodynamics of a conejet operated in a mixed ion-droplet regime, where ions are primarily emitted from the neck region where the highest normal electric field strengths occur.[2] The direction of the field gives the ions momentum away from the axis, consistent with the peaked distributions off axis. This is consistent with the ion energy distribution, which is narrow and centered at the needle potential. Thus, the ions have to be emitted from region along the conejet at high fields with no upstream ohmic losses, which can only be the neck. The droplets are produced on-axis consistent with droplet formation at the tip of the jet where the potential is lower due to ohmic losses that occur in the neck region. The observation of a lower and weaker ion energy component, on-axis and to a lesser degree at large angles, indicates that some ions are also produced either at the tip of the jet, or from the droplets. Ions formed at the tip of the jet would have lower energies and could experience repulsions from other ions or droplets of the same charge by Coulomb forces resulting in an off-axis distribution. The decrease in the relative intensity for the low energy component at large angles further points to the possibility that some ions could be emitted from the droplets. This ion emission would occur rapidly follow the formation of the droplets, in the vicinity of the tip of the jet where the gradient of acceleration field varies considerably. Ions are formed at lower potential than droplets because when released they have less kinetic energies.[13]

Interestingly, Lozano's higher resolution retarding energy analysis in pure ionic emission regime suggests that 10% of the beam current is carried away by metastable species that break up quickly after the extraction while inside the emitter accelerating region. Minor ionic species are also observed in the present study for both polarities. These minor trace ions are present at small angles where the droplets are dominant suggesting that these ions could originate from the droplets. The retarding energy curves of minor ions resemble those of the droplets indicating that trace ions are formed from the droplets immediately in the vicinity of the jet. Recently, Gamero-Castaño et al characterized the thrust current and retarding potential analyses with moving detectors in a capillary configuration. They found that ions and droplets co-existed in the core of the spray, while the outer region of the spray is depleted of ions.[14] The spray is found to have a 39.2 degree cone for a beam current of 260 nA. This is consistent with a mixed regime operated at a high flow rate where predominantly droplets are formed at the end of the jet and the observed ions were produced from the droplets in the center of the spray.

In contrast to the alternating polarity operation, the current output decays with time when the thruster is operated at positive dc mode. In addition, two new ion masses are observed and they are tentatively assigned to $EMI\text{-}Im^+$ and $[EMI\text{-}Im]^+[EMI\text{-}Im]$ ions associated with the electrochemical products. The Im adducts can be rationalized by the neutralization of Im on the needle which then binds with EMI^+, possibly through a proton or hydrogen-transfer complex. These electrochemical products are observed to be present at all angles, and their angular dependences resemble those of corresponding EMI^+ and $EMI^+[EMI\text{-}Im]$ ions, consistent with the formation of Im adducts. Also seen in Fig. 12 is the decrease of the fraction of the droplet background with time, which together with the decrease in the thruster current, is consistent with a throttled flow that favors ion evaporation over droplet formation. Very interesting is the observation that after several hours of operation in a dc mode, reverting to the ac polarity mode leads to instant recovery of the original current. These observations suggest that propellant fouling is not the main cause of the current reduction, but that an electrochemical modification of the liquid-metal interface effectively throttles the flow. One envisioned scenario is a steady built-up of charge layers with alternating polarities extending beyond the electrochemical double layer, thereby immobilizing a growing fraction of the liquid. Once the polarity is

reversed, the built-up interfacial structure disintegrates, and the layering of a new stack is initialized starting with the opposite polarity. "Quasi-ternary layers" have been proposed to clarify the capacitive behavior of imidazolium based ionic liquid.[15] The same study also found evidence for bulky, rough interface layers due to ionic cluster pairs, fully consistent with the present mass spectrometric observations.

Contrary to the observation from the positive dc mode, a time independent constant current is observed for the negative dc mode operation, and there is no evidence of electrochemical products. The possible oxidation reaction of $EMI^+ + e^-$ is likely to form imidazole radicals (i.e., carbenes) and small amounts of H_2 gas.[16] The formation of bubbles has been previously observed for EMI-BF_4.[8] The failure to observe complex anions formed between Im^- and shorted-lived imidazole radicals is not surprising.

V. Conclusion

Angularly resolved mass spectrometric measurements for EMI-Im wetted on a tungsten needle with energy analyses provide new insights into the ion emission mechanism of electrospray thrusters. The observations are consistent with an electrospray thruster operated in a mixed ion-droplet regime, where droplets are formed on-axis while ions are mostly found at large angles. Electrochemistry is effectively suppressed by operating in an alternating polarity mode. The thruster current declines when the wetted needle is operated at a positive dc mode. The observed current instability is not necessarily attributable to the electrochemical decay, but to an electrochemical modification of charge layers at the ionic liquid and metal interface, resulting in suppression of the propellant flow. The stable dc positive charge emission mode of the ST7 colloid thruster is most likely due to efficient removal of electrochemical products at the high propellant flow rates of the low I_{SP} system.

Acknowledgments

This work was supported by AFOSR through task 2303EO02 as part of the Space Miniaturization Theme (Program Manager: Michael Berman). The authors are greatly indebted to P. Lozano for his assistance in preparing the etched tungsten needles, and the fruitful discussion with M. Martínez-Sánchez (MIT) and J. Fernández de la Mora (Yale) regarding this work.

References

[1]Fernández de la Mora, J. and Loscertales, I. G., "The Current Emitted by Highly Conducting Taylor Cones," *Journal of Fluid Mechanics*, Vol. 260, 1994, pp. 155-184.

[2]Gamero-Castaño, M. and Fernández de la Mora, J., "Direct Measurement of Ion Evaporation Kinetics from Electrified Liquid Surfaces," *Journal of Chemical Physics*, Vol. 113, No. 2, 2000, pp. 815-832.

[3]Ziemer, J. K., Marrese-Reading, C. M., Anderson, M., Plett, G., Polk, J., Gamero-Castano, M., and Hruby, V., "Colloid Thruster Propellant Stability After Radiation Exposure." AIAA-2003-4853, 39th AIAA/ASME/SAE/ASEE Joint Propulsion Conference, Huntsville, AL, July 20-23, 2003.

[4]Gamero-Castaño, M., Hruby, V., Spence, D., Demmons, N., McCormick, R., Gasdaska, C., and Faulkos, P., "Micro Newoton Colloid Thruster for ST7-DRS Mission." AIAA-2003-4543, 39th AIAA/ASME/SAE/ASEE Joint Propulsion Conference, Huntsville, AL, July 20-23, 2003.

[5]Gamero-Castaño, M. and Hruby, V., "Electrospray as a Source of Nanoparticles for Efficient Colloid Thruster," *Journal of Propulsion and Power*, Vol. 17, No. 5, 2001, pp. 977-987.

[6]Lozano, P. C., "Energy Properties of an EMI-Im Ionic Liquid Ion Source," *Journal of Physics D: Applied Physics*, Vol. 39, 2006, pp. 126-134.

[7]Lozano, P. and Martínez-Sánchez, M., "Ionic Liquid Ion Sources: Characterization of Externally Wetted Emitters," *Journal of Colloid and Interface Science*, Vol. 282, 2005, pp. 415-421.

[8]Lozano, P. and Martínez-Sánchez, M., "Ionic Liquid Ion Sources: Suppression of Electrochemical Reactions Using Voltage Alternation," *Journal of Colloid and Interface Science*, Vol. 280, 2004, pp. 149-154.

[9]Ziemer, J. K., Gamero-Castaño, M., Hruby, V., Spence, D., Demmons, N., McCormick, R., Roy, T., Gasdaska, C., Young, J., and Connolly, B., "Colloid Micro-Newton Thruster Develpment for the ST7-DRS and LISA Missions." AIAA-2005-4265, 41st AIAA/ASME/SAE/ASEE Joint Propulsion Conference, Tucson, AZ, July 10-13, 2005.

[10]Lewandowski, A. and Galiński, M., "Carbon-ionic liquid double-layer Capacitors," *Journal of Physics and Chemistry of Solids*, Vol. 65, 2004, pp. 281-286.

[11]Chiu, Y., Austin, B. L., Dressler, R. A., Levandier, D. J., Murray, P. T., Lozano, P., and Martínez-Sánchez, M., "Mass Spectrometric Analysis of Colloid Thruster Ion Emission from Selected Propellants," *Journal of Propulsion and Power*, Vol. 21, No. 3, 2005, pp. 416-423.

[12]Chiu, Y. and Dressler, R. A., "Ionic Liquids for Space Propulsion," 231th American Chemical Society National Meeting, Atlanta, GA, March 26-30, 2006.

[13]Gamero-Castaño, M., "Electric-field-induced Ion Evaporation from Dielectric Liquid," *Physical Review Letters*, Vol. 89, No. 14, 2002, pp. 147602-147606.

[14]Gamero-Castaño, M., "Characterization of Colloid Thruster Beams", 3rd Nanoelectrojet /Colloid thruster workshop, Cambridge, MA, April 14-15, 2005.

[15]Liu, H., He, P., Li, Z., Liu, Y., Li, J., Zheng, L., and Li, J., "The Inherent Capacitive Behavior of Imidazolium-based Room-temperature Ionic Liquids at Carbon Paste Electrode," *Electrochemical and Solid State Letters*, Vol. 8, No. 7, 2005, pp. J17-J19.

[16]Squarez, P. A. Z., Consorti, C. S., Souza, R. F. d., Dupont, J., and Gonçalves, R. S., "Electrochemical Behavior of Vitreous Glass Carbon and Platinum Electrodes in the Ionic Liquid 1-*n*-butyl-3-methylimidazolium trifluoroacetate," *Journal of Brazilian Chemical Society*, Vol. 13, 2002, pp. 106-109.